Journal of Statistical Physics, Vol. 116, Nos. 1/4, August 2004 (© 2004)

Quantum Phase Diagram of an Exactly Solved Mixed Spin Ladder

M. T. Batchelor,[1] X.-W. Guan,[1] N. Oelkers,[1] and Z.-J. Ying[2]

Received August 13, 2003; accepted November 19, 2003

We investigate the quantum phase diagram of the exactly solved mixed spin-($\frac{1}{2}$, 1) ladder via the thermodynamic Bethe ansatz (TBA). In the absence of a magnetic field the model exhibits three quantum phases associated with $su(2)$, $su(4)$, and $su(6)$ symmetries. In the presence of a strong magnetic field, there is a third and full saturation magnetization plateaux within the strong antiferromagnetic rung coupling regime. Gapless and gapped phases appear in turn as the magnetic field increases. For weak rung coupling, the fractional magnetization plateau vanishs and the model undergoes new quantum phase transitions. However, in the ferromagnetic coupling regime, the system does not have a third saturation magnetization plateau. The critical behaviour in the vicinity of the critical points is also derived systematically using the TBA.

KEY WORDS: Mixed spin ladder; exactly solved model; magnetization plateaux; phase diagram.

1. INTRODUCTION

The field of exactly solved models in statistical mechanics has many significant highlights. These include Elliott Lieb's pioneering work on the six-vertex model and his calculation of the residual entropy of square ice.[1] Over the ensuing years the six-vertex model and the related Heisenberg spin chain have been generalised in all manner of directions. Most recently attention has turned to the physics of quantum spin ladders, for which

[1] Department of Theoretical Physics, Research School of Physical Sciences and Engineering, and Centre for Mathematics and its Applications, Mathematical Sciences Institute, Australian National University, Canberra ACT 0200, Australia; e-mail: murrayb@maths.anu.edu.au

[2] Instituto de Física da UFRGS, Av. Bento Gonçalves, 9500, Porto Alegre, 91501-970, Brasil and Hangzhou Teachers College, Hangzhou 310012, People's Republic of China.

0022-4715/04/0800-0571/0 © 2004 Plenum Publishing Corporation

a number of exactly solved models have been proposed. The underlying model is the spin-$\frac{1}{2}$ Heisenberg ladder, which has been studied extensively.[2] This model consists of two Heisenberg chains coupled together with Heisenberg rung interactions forming a ladder-like structure. A number of ladder compounds have been synthesized, such as $SrCu_2O_3$,[3] $Cu_2(C_5H_{12}N_2)_2Cl_4$,[4] $(C_5H_{12}N)_2CuBr_4$,[5] $(5IAP)_2CuBr_4 \cdot 2H_2O$,[6] $KCuCl_3$ and $TlCuCl_3$.[7] The experimental results reveal an interesting mix of low-temperature physics, including spin excitation gaps and magnetization plateaux.

The theoretical investigation of the ladder compounds has also been centred on a number of variants of the standard Heisenberg ladder,[8] including the addition of multi-body interactions,[9] alternation and frustration.[10, 11] The ladder models have been studied by a variety of methods, for example, numerical,[8, 12] perturbation theory,[13, 14] and the quantum transfer matrix algorithm.[15] Unfortunately the Heisenberg ladder is not exactly solvable in the sense of the six-vertex model or related $su(2)$ Heisenberg chain. However, a number of variants have been solved exactly by means of the Bethe ansatz; see, for example, refs. 16–21. For arguably the simplest model, based on $su(4)$, the critical behaviour derived from the thermodynamic Bethe ansatz (TBA) is seen to be consistent with the existing experimental, numerical and perturbative results for the strong coupling ladder compounds.[22] This includes the spin excitation gap and the critical fields H_{c1} and H_{c2}, which are in excellent agreement with the experimental values for the known strong coupling ladder compounds $(5IAP)_2CuBr_4 \cdot 2H_2O$, $Cu_2(C_5H_{12}N_2)_2Cl_4$ and $(C_5H_{12}N)_2CuBr_4$.

On the other hand, the special interest in fractional magnetization plateaux[23] has inspired work on mixed spin chains,[24–27] mixed spin ladders,[28] and various experimental compounds.[29–31] In particular, the magnetic behaviour of a mixed spin-($\frac{1}{2}$, 1) Heisenberg ladder has been investigated by means of the density-matrix renormalization group technique.[28] It was concluded that for certain strong rung coupling magnetization plateaux exist at $M^z = 0.5$ and at $M^z = 1$, but with no plateaux for negative (ferromagnetic) rung coupling. In fact the mixed spin ladder exhibits a richer phase diagram than the spin-$\frac{1}{2}$ ladder. It appears that a comprehensive study of the mixed spin ladder, e.g., the prediction of the critical fields for different rung coupling and examination of the critical behavior, has not been undertaken. It also remains to investigate the effect of non-equal Landé g-factors on the ladder legs, particularly given that g-factor anisotropy appears to affect the critical fields in the spin-orbital model.[32, 33]

In this paper, we investigate the quantum phase diagram of the exactly solved mixed spin-($\frac{1}{2}$, 1) ladder,[19] with different g-factors, via the TBA. We find that in the absence of a magnetic field the model exhibits three

quantum phases associated with $su(2)$, $su(4)$, and $su(6)$ symmetries. In the presence of a strong magnetic field h, two magnetization plateaux appear in the strong antiferromagnetic rung coupling regime. The fractional magnetization plateau $M^z = \frac{1}{2} g_s \mu_B + \frac{1}{6} (g_s - g_t) \mu_B$ corresponding to the fully-polarized doublet rung state, opens at the critical field H_{c1} and vanishes at the critical field H_{c2}. The second plateau $M^z = (\frac{1}{2} g_t + g_s) \mu_B$, corresponding to a fully-polarized quadruplet rung state, opens only at a very strong magnetic field H_{c3}. For weak antiferromagnetic rung coupling, the fractional plateau is closed such that three different kinds of quantum phase transition occur. For ferromagnetic rung coupling only the full saturation magnetization plateau exists. The critical behavior for the different quantum phase transitions is systematically derived by using the TBA.

The paper is organized as follows. In Section 2, we discuss the exactly solved mixed spin-($\frac{1}{2}$, 1) ladder model with different Landé factors. The exact solution is given via an appropriate choice of rung basis. Section 3 is devoted to the investigation of the quantum phase diagram. In Section 4 we investigate the magnetization plateaux in the presence of a strong magnetic field. The critical fields characterizing the different quantum phase transitions are given explicitly. A summary of our main results and conclusions are given in Section 5.

2. THE EXACTLY SOLVED MIXED SPIN-($\frac{1}{2}$, 1) LADDER MODEL

The Hamiltonian of the exactly solved spin-($\frac{1}{2}$, 1) ladder model, based on the $su(6)$ symmetry, reads[19]

$$H = J_{\parallel} H_{\text{leg}} + J_{\perp} \sum_{j=1}^{L} \vec{T}_j \cdot \vec{S}_j - g_t \mu_B h \sum_{j=1}^{L} T_j^z - g_s \mu_B h \sum_{j=1}^{L} S_j^z, \tag{1}$$

$$H_{\text{leg}} = \sum_{j=1}^{L} (\tfrac{1}{2} + 2 \vec{T}_j \cdot \vec{T}_{j+1}) (-1 + \vec{S}_j \cdot \vec{S}_{j+1} + (\vec{S}_j \cdot \vec{S}_{j+1})^2). \tag{2}$$

Here $\vec{T}_j$ and $\vec{S}_j$ are the standard spin-$\frac{1}{2}$ and spin-1 operators acting on site j of the upper and lower legs, respectively (see Fig. 1), $J_{\parallel}$ and $J_{\perp}$ are the intrachain and interchain coupling constants, h is the magnetic field, μ_B is the Bohr magneton and g_t and g_s are the Landé factors along each leg. Periodic boundary conditions are imposed with L the number of rungs.

The rung term in (1) breaks the $su(6)$ symmetry of H_{leg} into $su(4) \oplus u(2)$ symmetry. This symmetry is in turn broken under the magnetic field. The physical properties and the critical behaviour of the model are determined by the competition between the rung and leg coupling constants

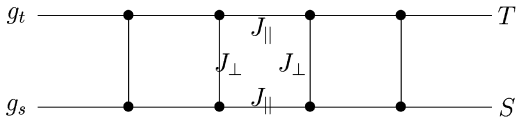

Fig. 1. The mixed spin ladder: $J_\parallel$ and $J_\perp$ are the intrachain and interchain couplings; g_t and g_s are the Landé factors along each leg.

and the magnetic field h. Essentially, H_{leg} is the permutation operator corresponding to the $su(6)$ algebra symmetry. If we change the canonical basis $e_i^{\alpha\beta} \otimes e_j^{\gamma\delta}$ of $V_1 \otimes V_2$ into rung quadruplet and doublet states (Clebsch–Gordan decomposition), the six-dimensional space splits into the direct sum of quadruplets and doublets with the basis

$$
\begin{aligned}
|1\rangle &= \tfrac{\sqrt{2}}{\sqrt{3}}\left(|1, -\tfrac{1}{2}\rangle - \tfrac{1}{\sqrt{2}}\,|0, \tfrac{1}{2}\rangle\right), & |2\rangle &= \tfrac{\sqrt{2}}{\sqrt{3}}\left(|-1, \tfrac{1}{2}\rangle - \tfrac{1}{\sqrt{2}}\,|0, -\tfrac{1}{2}\rangle\right), \\
|3\rangle &= |1, \tfrac{1}{2}\rangle, & |4\rangle &= \tfrac{1}{\sqrt{3}}\left(|1, -\tfrac{1}{2}\rangle + \sqrt{2}\,|0, \tfrac{1}{2}\rangle\right), \\
|5\rangle &= \tfrac{1}{\sqrt{3}}\left(|-1, \tfrac{1}{2}\rangle + \sqrt{2}\,|0, -\tfrac{1}{2}\rangle\right), & |6\rangle &= |-1, -\tfrac{1}{2}\rangle,
\end{aligned}
\tag{3}
$$

where the states $|1\rangle, |2\rangle$ form the doublet and the remaining states form the quadruplet. The projectors onto the doublet and quadruplet subspace are given by

$$
P_{\text{d}} = -\tfrac{2}{3}\left(\vec{T}\cdot\vec{S} - \tfrac{1}{2}\right), \qquad P_{\text{q}} = \tfrac{2}{3}\left(\vec{T}\cdot\vec{S} + 1\right). \tag{4}
$$

It follows that the rung interaction term can be accommodated into an $su(6)$ invariant Heisenberg chain by embedding the doublet rung states through an appropriate chemical potential term. The leg and rung part of the Hamiltonian (1) can be derived from the relation

$$
H = J_\parallel \frac{d}{dv} \ln \tau(v)|_{v=0} + E_{\perp+h} + \text{const} \tag{5}
$$

associated with the quantum transfer matrix $\tau(v) = \text{tr}_0\, T(v)$. The energy $E_{\perp+h}$ arising from the rung interaction and magnetic field terms is given further below. Here $T(u)$ denotes the monodromy matrix given by

$$
T(v) = R_{0,L}(v)\, R_{0,L-1}(v) \cdots R_{0,2}(v)\, R_{0,1}(v) \tag{6}
$$

associated with the $su(6)$ quantum R-matrix.

Now consider the effect of the magnetic field. Although the magnetic field preserves the integrability of the leg part of the Hamiltonian, the different g-factors on each leg break the doublet/quadruplet basis (3) for the Hamiltonian (1). Fortunately, we can still find another basis,

$$\begin{aligned}
\psi_{\frac{1}{2}}^{(\pm)} &= \frac{1}{\sqrt{1+(y_{\frac{1}{2}}^{(\pm)})^2}}\,(|1,-\tfrac{1}{2}\rangle + y_{\frac{1}{2}}^{(\pm)}\,|0,\tfrac{1}{2}\rangle),\\
\psi_{-\frac{1}{2}}^{(\pm)} &= \frac{1}{\sqrt{1+(y_{-\frac{1}{2}}^{(\pm)})^2}}\,(|-1,\tfrac{1}{2}\rangle + y_{-\frac{1}{2}}^{(\pm)}\,|0,-\tfrac{1}{2}\rangle),\\
\psi_{\frac{3}{2}} &= |1,\tfrac{1}{2}\rangle, \qquad \psi_{-\frac{3}{2}} = |-1,-\tfrac{1}{2}\rangle,
\end{aligned} \tag{7}$$

to diagonalize the rung and magnetization terms simultaneously. The quantities $y_a^{(\pm)}$ are given by

$$y_a^{(\pm)} = a\sqrt{2}\,[(g_s - g_t)\,h' + a] \pm \sqrt{1+\tfrac{1}{2}\,(g_s h' - g_t h' + a)^2}\,, \tag{8}$$

where $a = \pm\frac{1}{2}$ and $h' = \mu_B h/J_\perp$. We notice that if $g_s = g_t$, the basis states $\psi_{\frac{1}{2}}^{(-)}$ and $\psi_{-\frac{1}{2}}^{(-)}$ reduce to the doublet, with the other states reducing to the quadruplet. With regard to the total spin of the multiplets we can still call the states $(\psi_{\frac{3}{2}}, \psi_{\frac{1}{2}}^{(+)}, \psi_{-\frac{1}{2}}^{(+)}, \psi_{-\frac{3}{2}})$ quadruplets and $(\psi_{\frac{1}{2}}^{(-)}, \psi_{-\frac{1}{2}}^{(-)})$ doublets.

It is well established that the Hamiltonian (1) can be diagonalized via the algebraic Bethe ansatz. In this procedure it is important to note that the leg content of the Hamiltonian, H_{leg}, is not altered under the change of basis order between the quadruplet and the doublet states, however the rung and magnetic field terms are altered by these changes. We note also that for the ladder Hamiltonian (1) the doublet rung state is energetically favoured for $J_\perp > 0$, whereas the quadruplet rung state is favoured for $J_\perp < 0$. This is the reason for choosing the doublet state as reference state for $J_\perp > 0$, while a quadruplet state is choosen as reference state for $J_\perp < 0$. As the magnetic field is turned on, the energy levels of each multiplet component split. The basis order is therefore chosen in accordance with their energy levels.

The resulting Bethe ansatz equations are well known[34] and consist of a set of five coupled equations depending on five flavours, $v^{(k)}$, $k = 1,\ldots, 5$. The Bethe ansatz equations

$$\prod_{\ell=1}^{M_{k-1}} \frac{v_j^{(k)} - v_\ell^{(k-1)} + \frac{\mathrm{i}}{2}}{v_j^{(k)} - v_\ell^{(k-1)} - \frac{\mathrm{i}}{2}} = \prod_{\substack{l=1\\ l\neq j}}^{M_k} \frac{v_j^{(k)} - v_l^{(k)} + \mathrm{i}}{v_j^{(k)} - v_l^{(k)} - \mathrm{i}} \prod_{l=1}^{M_{k+1}} \frac{v_j^{(k)} - v_l^{(k+1)} - \frac{\mathrm{i}}{2}}{v_j^{(k)} - v_l^{(k+1)} + \frac{\mathrm{i}}{2}} \tag{9}$$

can be derived from the nested algebraic Bethe ansatz. In the above, $k = 1,..., 5$ and $j = 1,..., M_k$ and the conventions $v_j^{(0)} = v_j^{(6)} = 0, M_6 = 0$ apply. In real ladder compounds the difference between the g-factors along each leg is small (this is not always true for spin-orbital models[32]). Thus from now on we treat the term $g_s - g_t$ as a small quantity. After some algebra, the eigenspectrum is obtained from relation (5) as

$$E = J_\parallel L - J_\parallel \sum_{i=1}^{M_1} \frac{1}{v_i^2 + \frac{1}{4}} + E_{\perp+h}, \tag{10}$$

where $v_j = v_j^{(1)}$ and the energy contribution from the rung interaction and the magnetic field terms is given by

$$\begin{aligned}
E_{\perp+h} = &\left[-\frac{1}{4} J_\perp - \frac{1}{2} g_s \mu_B h - \frac{1}{\sqrt{2}} J_\perp \sqrt{1 + \frac{1}{2}\left(g_s h' - g_t h' + \frac{1}{2} \right)^2} \right] N_{\frac{1}{2}}^{(-)} \\
&+ \left[-\frac{1}{4} J_\perp + \frac{1}{2} g_s \mu_B h - \frac{1}{\sqrt{2}} J_\perp \sqrt{1 + \frac{1}{2}\left(g_s h' - g_t h' - \frac{1}{2} \right)^2} \right] N_{-\frac{1}{2}}^{(-)} \\
&+ \left[\frac{1}{2} J_\perp - \left(\frac{1}{2} g_t + g_s \right) \mu_B h \right] N_{\frac{3}{2}} \\
&\times \left[-\frac{1}{4} J_\perp - \frac{1}{2} g_s \mu_B h + \frac{1}{\sqrt{2}} J_\perp \sqrt{1 + \frac{1}{2}\left(g_s h' - g_t h' + \frac{1}{2} \right)^2} \right] N_{\frac{1}{2}}^{(+)} \\
&+ \left[-\frac{1}{4} J_\perp + \frac{1}{2} g_s \mu_B h + \frac{1}{\sqrt{2}} J_\perp \sqrt{1 + \frac{1}{2}\left(g_s h' - g_t h' - \frac{1}{2} \right)^2} \right] N_{-\frac{1}{2}}^{(+)} \\
&+ \left[\frac{1}{2} J_\perp + \left(\frac{1}{2} g_t + g_s \right) \mu_B h \right] N_{-\frac{3}{2}} \\
= &\left[-\frac{3}{2} J_\perp - \frac{1}{2} g_s \mu_B h - \frac{1}{6} (g_s - g_t) \mu_B h \right] N_{\frac{1}{2}}^{(-)} \\
&+ \left[-\frac{3}{2} J_\perp + \frac{1}{2} g_s \mu_B h + \frac{1}{6} (g_s - g_t) \mu_B h \right] N_{-\frac{1}{2}}^{(-)} \\
&- \left(\frac{1}{2} g_t + g_s \right) \mu_B h N_{\frac{3}{2}} - \left[\frac{1}{2} g_s \mu_B h - \frac{1}{6} (g_s - g_t) \mu_B h \right] N_{\frac{1}{2}}^{(+)} \\
&+ \left[\frac{1}{2} g_s \mu_B h - \frac{1}{6} (g_s - g_t) \mu_B h \right] N_{-\frac{1}{2}}^{(+)} \\
&+ \left(\frac{1}{2} g_t + g_s \right) \mu_B h N_{-\frac{3}{2}} + \text{const.}
\end{aligned} \tag{11}$$

Here the N's are the numbers of the corresponding states. In the thermodynamic limit, the Bethe ansatz equations (9) allow the string solution[35, 36]

$$v^{(k)}{}^{n}_{\alpha_k j} = v^{(k)}{}^{n}_{\alpha_1} + \tfrac{1}{2}\,\mathrm{i}(n+1-2j), \tag{12}$$

where $j = 1,..., n$, $\alpha_a = 1,..., N_n^{(k)}$ and $v^{(k)n}_{\alpha_k}$, $k = 1,..., 5$, are the positions of the center of the strings of flavour k. The number of n-strings, $N_n^{(a)}$, satisfies the relation $M^{(k)} = \sum_n nN_n^{(k)}$. On taking the thermodynamic limit, the Bethe ansatz equations become

$$\rho_n^{(1)\,h} = a_n - \sum_m A_{nm} * \rho_m^{(1)} + \sum_m a_{nm} * \rho_m^{(2)}, \tag{13}$$

$$\rho_n^{(k)\,h} = -\sum_m A_{nm} * \rho_m^{(k)} + \sum_m a_{nm} * (\rho_m^{(k-1)} + \rho_m^{(k+1)}), \tag{14}$$

where $k = 2,..., 5$, and the symbol $*$ denotes convolution. $\rho_n^{(k)}(v)$ and $\rho_n^{(k)\,h}(v)$ with $k = 1,..., 5$ are the densities of roots and holes for the five flavours. We have adopted the standard notations

$$A_{nm}(\lambda) = \delta(\lambda)\,\delta_{nm} + (1-\delta_{nm})\,a_{|n-m|}(\lambda) + a_{n+m}(\lambda) + 2\sum_{l=1}^{\mathrm{Min}(n,\,m)-1} a_{|n-m|+2l}(\lambda), \tag{15}$$

$$a_{nm}(\lambda) = \sum_{l=1}^{\mathrm{Min}(n,\,m)} a_{n+m+1-2l}(\lambda), \tag{16}$$

with $a_n(\lambda) = \frac{1}{2\pi}\frac{n}{n^2/4+\lambda^2}$.

In order to find the equilibrium state of the system at a fixed temperature T and external magnetic field $h \geqslant 0$, we minimize the free energy $F = E - TS - hM^z$ with respect to the densities and then obtain the TBA equations in the form

$$\epsilon_1^{(k)} = g_1^{(k)} + Ta_2 * \ln(1+e^{-\frac{\epsilon_1^{(k)}}{T}}) + T(a_0+a_2)\sum_{m=1}^{\infty} a_m * \ln(1+e^{-\frac{\epsilon_{m+1}^{(k)}}{T}}) - T\sum_{m=1}^{\infty} a_m * \left(\ln(1+e^{-\frac{\epsilon_m^{(k-1)}}{T}}) + \ln(1+e^{-\frac{\epsilon_m^{(k+1)}}{T}})\right), \tag{17}$$

$$\epsilon_n^{(k)} = g_n^{(k)} + Ta_1 * \ln(1+e^{\frac{\epsilon_{n-1}^{(k)}}{T}} + Ta_2 * \ln(1+e^{-\frac{\epsilon_n^{(k)}}{T}})) + T(a_0+a_2)\sum_{m\geqslant n}^{\infty} a_{m-n} * \ln(1+e^{-\frac{\epsilon_m^{(k)}}{T}}) - T\sum_{m\geqslant n}^{\infty} a_{m-n+1} * \left(\ln(1+e^{-\frac{\epsilon_m^{(k-1)}}{T}}) + \ln(1+e^{-\frac{\epsilon_m^{(k+1)}}{T}})\right), \qquad n \geqslant 2. \tag{18}$$

Here $\rho_n^{(k)\,h}(\lambda)/\rho_n^{(k)}(\lambda) := \exp(\epsilon_n^{(k)}(\lambda)/T)$ with $k = 1,..., 5$ and $\epsilon_n^{(0)}(\lambda) = \epsilon_n^{(6)}(\lambda) = 0$ is assumed. The dressed energies $\epsilon_n^{(k)}$ play the role of excitation energies measured from the Fermi level for each flavour. The driving terms in the antiferromagnetic rung coupling regime for a weak magnetic field, $h < \frac{3J_\perp}{[g_t+3g_s+(g_s-g_t)/3]\,\mu_B}$, are given by

$$
\begin{aligned}
g_1^{(1)} &= -J_\parallel \frac{1}{v^2+\frac{1}{4}} + \left[g_s + \frac{1}{3}(g_s - g_t) \right] \mu_B h, \\
g_1^{(2)} &= \frac{3}{2} J_\perp - \left[\frac{1}{2} g_t + \frac{3}{2} g_s + \frac{1}{6}(g_s - g_t) \right] \mu_B h, \\
g_1^{(3)} &= \left[\frac{1}{2}(g_t + g_s) + \frac{1}{6}(g_s - g_t) \right] \mu_B h, \\
g_1^{(4)} &= \left[g_s - \frac{1}{3}(g_s - g_t) \right] \mu_B h, \\
g_1^{(5)} &= \left[\frac{1}{2}(g_t + g_s) + \frac{1}{6}(g_s - g_t) \right] \mu_B h.
\end{aligned} \tag{19}
$$

The higher driving terms are given by $g_n^{(1)} = n[g_s + \frac{1}{3}(g_s - g_t)]\,\mu_B h$ and $g_n^{(k)} = n g_1^{(k)}$ for $k > 1$. Consequently, the free energy is given by

$$
\begin{aligned}
\frac{f(h,T)}{L} = &-\frac{1}{2} g_s \mu_B h - \frac{1}{6}(g_s - g_t)\,\mu_B h \\
&- T \int_{-\infty}^{\infty} \sum_{n=1}^{\infty} a_n(\lambda) \ln(1 + e^{-\frac{\epsilon_n^{(1)}(\lambda)}{T}})\, d\lambda.
\end{aligned} \tag{20}
$$

It is worth mentioning that the driving terms vary for different choices of the basis order. The TBA equations (17) and (19) provide a clear physical picture of the groundstate and make the thermodynamic properties, such as the free energy, magnetization and susceptibility accessible.

3. QUANTUM PHASE DIAGRAM

In the low temperature limit, the states with positive dressed energy are empty. The rapidities with negative dressed energy correspond to occupied states. The zeros of the dressed energies define the Fermi energies. As usual, we decompose $\epsilon_n^{(a)}$ into positive and negative parts, $\epsilon_n^{(k)} = \epsilon_n^{(k)+} + \epsilon_n^{(k)-}$, with only the negative dressed energies contributing to the groundstate energy. Analysis of Eqs. (17) and (19) in the limit $T \to 0$

reveals that the roots are all real for the groundstate, corresponding to $n=1$. All dressed energies $\epsilon_n^{(k)+}$ with $n \geqslant 2$ correspond to excitations. Under this circumstance, we see that all energy bands are completely filled in the absence of an external magnetic field and rung interactions.

In order to derive the groundstate properties, we first consider the antiferromagnetic regime $J_\perp > 0$, where the doublet component $\psi_{\frac{1}{2}}^{(-)}$ is chosen as the reference state with a basis order ($\psi_{\frac{1}{2}}^{(-)}$, $\psi_{-\frac{1}{2}}^{(-)}$, $\psi_{\frac{3}{2}}$, $\psi_{\frac{1}{2}}^{(+)}$, $\psi_{-\frac{1}{2}}^{(+)}$, $\psi_{-\frac{3}{2}}$). The groundstate TBA equations then read

$$\begin{aligned}
\epsilon^{(1)} &= g_1^{(1)} - a_2 * \epsilon^{(1)-} + a_1 * \epsilon^{(2)-}, \\
\epsilon^{(k)} &= g_1^{(k)} - a_2 * \epsilon^{(k)-} + a_1 * [\epsilon^{(k-1)-} + \epsilon^{(k+1)-}], \\
&\quad k = 2,\ldots, 5.
\end{aligned} \tag{21}$$

It is clear that without a magnetic field the $su(6)$ multiplet levels split due to the rung coupling. If $J_\perp$ is very large (the limit of strong rung coupling), the whole quadruplet state ($\psi_{\frac{3}{2}}, \psi_{\frac{1}{2}}^{(+)}, \psi_{-\frac{1}{2}}^{(+)}, \psi_{-\frac{3}{2}}$) is gapfull, i.e., $\epsilon^{(k)} > 0$ for $k > 2$. This means that the quadruplet is not involved in the groundstate—the groundstate consists of doublet states with massless excitation. From the TBA equation (21), we find that the quadruplet excitation gap is given by $\Delta_1 = \frac{3}{2} J_\perp - 2J_\parallel \ln 2$. Thus if $J_\perp$ becomes larger than the critical value $J_c^+ = \frac{4}{3} J_\parallel \ln 2$, there is a quantum phase transition from the Luttinger liquid $su(4) \oplus su(2)$ phase into the $su(2)$ phase. However, in the presence of a magnetic field this critical point is not stable. In this case the dressed energy levels become completely split by the magnetic field h. If the rung coupling $J_\perp$ is large enough so that the driving term $g_1^{(2)}$ in (19) remains positive, the quadruplet state could be gapfull and the groundstate would still be the doublet. However, as the magnetic field increases, the doublet component $\psi_{-\frac{1}{2}}^{(-)}$ gradually shifts out of the groundstate as the Fermi surface of the dressed energy $\epsilon^{(1)}$ lifts. Subsequently, if the magnetic field h is larger than the critical point H_{c1}, the reference state becomes a true physical state such that the strong rung coupling forms a rung trimerized groundstate (see Fig. 2). In other words, the doublet component $\psi_{\frac{1}{2}}^{(-)}$ forms a ferrimagnetic groundstate. The critical field H_{c1} is given by

$$H_{c1} = 4J_\parallel / [g_s + \tfrac{1}{3}(g_s - g_t)]\, \mu_B. \tag{22}$$

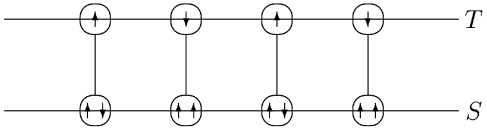

Fig. 2. The doublet polarized state forms a rung trimerized groundstate.

The critical point H_{c1} indicates a quantum phase transition from a gapless magnetic phase into a ferrimagnetic phase with gap $\Delta_2 = (\frac{1}{2}g_s + \frac{1}{6}(g_s - g_t)]\,\mu_B(h - H_{c1})$. It is worth noting that in this ferromagnetic phase a magnetization plateau $M^z = \frac{1}{2}g_s\mu_B + \frac{1}{6}(g_s - g_t)\,\mu_B$ opens. The necessary condition for this plateau to exist is

$$J_\perp \geqslant J_c^{+F} = \frac{8J_\parallel}{3}\frac{[\frac{1}{2}g_t + \frac{3}{2}g_s + \frac{1}{6}(g_s - g_t)]}{[g_s + \frac{1}{3}(g_s - g_t)]}. \tag{23}$$

In the critical phase $h < H_{c1}$, the TBA equations with a very large or a very small Fermi boundary can be solved analytically. If the magnetic field is very small, i.e., $h \ll 1$, the Fermi boundary of the dressed energy $\epsilon^{(1)}$ is very large. The energy potential satisfies the Wiener–Hopf type equation

$$\epsilon^{(1)}(\lambda) = -J_\parallel\frac{\pi}{\cosh \pi\lambda} + \frac{1}{2}\left[g_s + \frac{1}{3}(g_s - g_t)\right]\mu_B h + \int_{-\infty,\,B}^{-B,\,\infty} G(\lambda - k) * \epsilon^{(1)}(k)\,dk. \tag{24}$$

Here the function $G(\lambda)$ is defined via

$$G(\lambda) = \frac{1}{2\pi}\int_{-\infty}^{\infty}\frac{e^{-|\omega|/2}}{2\cosh \omega/2}e^{-i\lambda\omega}\,d\omega.$$

Using the standard Wiener–Hopf technique, we find that the Fermi boundary satisfies the relation $e^{-B\pi} = [g_s + \frac{1}{3}(g_s - g_t)]\,\mu_B h a_-(0)/4J_\parallel \pi a_+(i\pi)$, where the decomposition functions are given by

$$a_+(\omega) = a_-(-\omega) = \sqrt{2}\,\pi\left(\frac{\eta - i\omega}{2\pi e}\right)^{-\frac{i\omega}{2\pi}}\Big/\Gamma\left(\frac{1}{2} - \frac{i\omega}{2\pi}\right). \tag{25}$$

The Fermi boundary decreases monotonically with increasing magnetic field. Correspondingly, the free energy is given by

$$\frac{F(0,h)}{L} \approx -J_\parallel\left[\Psi(1) - \Psi\left(\frac{1}{2}\right)\right] - \frac{1}{8\pi^2}\left[g_s + \frac{1}{3}(g_s - g_t)\right]^2\mu_B^2 h^2, \tag{26}$$

which suggests a susceptibility of $\chi \approx \frac{1}{4\pi^2}[g_s + \frac{1}{3}(g_s - g_t)]^2\,\mu_B^2$, indicating an $su(2)$ critical phase. In the above $\Gamma(z)$ and $\Psi(a)$ are the gamma and diagamma functions, respectively.

On the other hand, if the magnetic field h tends to the critical point H_{c1}, the Fermi boundary Q of the dressed energy $\epsilon^{(1)}$ is very small, say $Q \ll 1$ for $H_{c1} - h \ll 1$. Under this circumstance, the free energy is given by

$$\frac{F(0,h)}{L} \approx -\frac{1}{2}\left[g_s + \frac{1}{3}(g_s - g_t)\right]\mu_B h - \frac{4Q}{\pi}\left[g_s + \frac{1}{3}(g_s - g_t)\right]\mu_B(H_{c1} - h), \tag{27}$$

where $Q \approx \sqrt{(H_{c1}-h)/4H_{c1}}$. Thus the susceptibility

$$\chi \approx \frac{(4g_s - g_t)\,\mu_B}{\pi\sqrt{4H_{c1}}}\,(H_{c1}-h)^{-\frac{1}{2}} \tag{28}$$

indicates the singular behavior of the transition from the gapless phase into the gapped phase. In addition, from the Bethe ansatz equations and the relation

$$M^z \approx \tfrac{1}{2}g_s\mu_B + \tfrac{1}{6}(g_s - g_t)\,\mu_B - [g_s + \tfrac{1}{3}(g_s - g_t)]\,\mu_B \int_{-Q}^{Q} \rho_1^{(1)}(\lambda)\,d\lambda, \tag{29}$$

the magnetization per site M^z in the vicinity of H_{c1} follows as

$$M^z = \frac{1}{2}g_s\mu_B + \frac{1}{6}(g_s - g_t)\,\mu_B - \frac{4Q}{\pi}\left[g_s + \frac{1}{3}(g_s - g_t)\right]\mu_B\left(1 - \frac{2Q}{\pi}\right). \tag{30}$$

Apparently, as $h \to H_{c1}$ the magnetization M^z tends to the plateau value $\frac{1}{2}g_s\mu_B + \frac{1}{6}(g_s - g_t)\,\mu_B$. We shall discuss the magnetization plateaux as well as the quantum phase transitions in the next section.

For the ferromagnetic regime $J_\perp < 0$, the rung quadruplet component $\psi_{\frac{3}{2}}$ is chosen as the reference state with $(\psi_{\frac{3}{2}}, \psi_{\frac{1}{2}}^{(+)}, \psi_{-\frac{1}{2}}^{(+)}, \psi_{-\frac{3}{2}}, \psi_{\frac{1}{2}}^{(-)}, \psi_{-\frac{1}{2}}^{(-)})$ as the order of the basis. Thus the driving terms are given by

$$\begin{aligned}
g_1^{(1)} &= -J_\parallel \frac{1}{v^2 + \frac{1}{4}} + \left[\frac{1}{2}(g_t + g_s) + \frac{1}{6}(g_s - g_t)\right]\mu_B h,\\
g_1^{(2)} &= \left[g_s - \frac{1}{3}(g_s - g_t)\right]\mu_B h,\\
g_1^{(3)} &= \left[\frac{1}{2}(g_t + g_s) + \frac{1}{6}(g_s - g_t)\right]\mu_B h,\\
g_1^{(4)} &= -\frac{3}{2}J_\perp - \left[\frac{1}{2}g_t + \frac{3}{2}g_s + \frac{1}{6}(g_s - g_t)\right]\mu_B h,\\
g_1^{(5)} &= \left[g_s + \frac{1}{3}(g_s - g_t)\right]\mu_B h.
\end{aligned} \tag{31}$$

In the absence of a magnetic field, the quadruplet and doublet states are degenerate. If the rung coupling becomes negative enough the doublet state is completely gapfull, and the Fermi boundaries of the quadruplet states are infinite. Using Fourier transforms, we find that the doublet does not exist in the groundstate for $J_\perp < J_c^- = -\frac{2}{3}J_\parallel$. Again this critical point is

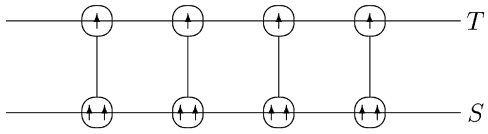

Fig. 3. The quadruplet fully-polarized state forms a trimerized ferromagnetic groundstate.

not stable if the magnetic field is applied. We can see that the Fermi surfaces of the dressed energies $\epsilon^{(k)}$, $k = 1, 2, 3$ lift, while the Fermi surfaces of the doublet sink. If the magnetic field is strong enough, i.e., if

$$h \geqslant h_c^- = 4J_\parallel / [\tfrac{1}{2}(g_t + g_s) + \tfrac{1}{6}(g_s - g_t)]\, \mu_{\mathrm{B}}, \tag{32}$$

the reference state $\psi_{\frac{3}{2}}$ becomes a true physical state. Thus the groundstate is a fully-polarized (trimer-like) ferromagnetic state (see Fig. 3). Note that the rung coupling $J_\perp$ must be less than a critical value $J_\perp^{-F}$ given by

$$J_\perp^{-F} = -\frac{8J_\parallel}{3} \frac{[\tfrac{1}{2} g_t + \tfrac{3}{2} g_s + \tfrac{1}{6}(g_s - g_t)]}{[\tfrac{1}{2}(g_t + g_s) + \tfrac{1}{6}(g_s - g_t)]}. \tag{33}$$

4. MAGNETIZATION PLATEAUX

Magnetization plateaux are one of the most interesting phenomena in the ladder compounds. For example, fractional magnetization plateaux have been found in Shastry–Sutherland systems.[37] Theoretical studies and numerical results suggest that magnetization plateaux exist in the mixed spin-($\frac{1}{2}$, 1) chains[24–26] and the mixed ladder.[28] From the analysis of the critical points of the solvable model in the last section, we found that gapped or gapless states appear in turn as the external magnetic field increases. For very strong rung coupling, i.e., $J_\perp \gg J_c^{+F}$, the two-component massless quantum magnetic phase lies in the regime $h < H_{c1}$. The ferrimagnetic phase appears for a magnetic field $h > H_{c1}$ and the component $\psi_{\frac{1}{2}}^{(-)}$ becomes a physical ferrimagnetic groundstate. On the other hand, the magnetic field can bring the state $\psi_{\frac{3}{2}}$ close to the groundstate. Eventually it becomes involved in the groundstate when the magnetic field is strong enough. From the expression (11), we see that if $h > 3J_\perp / (g_t + 3g_s + \frac{1}{3}(g_s - g_t))\, \mu_{\mathrm{B}}$, the state $\psi_{\frac{3}{2}}$ becomes an energetically lower lying state than $\psi_{-\frac{1}{2}}^{(-)}$. In this case it is convenient to reorder the basis as $(\psi_{\frac{1}{2}}^{(-)}, \psi_{\frac{3}{2}}, \psi_{-\frac{1}{2}}^{(-)}, \psi_{\frac{1}{2}}^{(+)}, \psi_{-\frac{1}{2}}^{(+)}, \psi_{-\frac{3}{2}})$. Here the TBA driving terms are given by

$$
\begin{aligned}
g_1^{(1)} &= -J_{\parallel}\frac{1}{v^2+\frac{1}{4}}+\frac{3}{2}J_{\perp}-\left[\frac{1}{2}(g_t+g_s)-\frac{1}{6}(g_s-g_t)\right]\mu_{\mathrm{B}}h,\\
g_1^{(2)} &= -\frac{3}{2}J_{\perp}+\left[\frac{1}{2}g_t+\frac{3}{2}g_s+\frac{1}{6}(g_s-g_t)\right]\mu_{\mathrm{B}}h,\\
g_1^{(3)} &= \frac{3}{2}J_{\perp}-g_s\mu_{\mathrm{B}}h,\\
g_1^{(4)} &= \left[g_s-\frac{1}{3}(g_s-g_t)\right]\mu_{\mathrm{B}}h,\\
g_1^{(5)} &= \left[\frac{1}{2}(g_t+g_s)+\frac{1}{6}(g_s-g_t)\right]\mu_{\mathrm{B}}h.
\end{aligned}
\tag{34}
$$

Analysing the TBA with these driving terms, we find that the ferrimagnetic groundstate can be maintained only in the regime $H_{c1}\leqslant h<H_{c2}$, where the critical point H_{c2} is given by

$$
H_{c2}=\frac{3J_{\perp}-8J_{\parallel}}{[(g_t+g_s)-\frac{1}{3}(g_s-g_t)]\,\mu_{\mathrm{B}}}. \tag{35}
$$

Beyond the critical field H_{c2}, the plateau $M^z=\frac{1}{2}g_s\mu_{\mathrm{B}}+\frac{1}{6}(g_s-g_t)\,\mu_{\mathrm{B}}$ vanishes. In the vicinity of H_{c2}, i.e., $h-H_{c2}\ll 1$, the Fermi boundary is very small. After a similar calculation the Fermi point is found to be

$$
Q\approx\sqrt{\frac{[\frac{1}{2}(g_t+g_s)-\frac{1}{6}(g_s-g_t)]\,\mu_{\mathrm{B}}(h-H_{c2})}{16J_{\parallel}}}\,. \tag{36}
$$

The susceptibility is given by

$$
\chi\approx\frac{3[\frac{1}{2}(g_s+g_t)\,\mu_{\mathrm{B}}-\frac{1}{6}(g_s-g_t)\,\mu_{\mathrm{B}}]^{\frac{3}{2}}}{4\pi\sqrt{J_{\parallel}(h-H_{c2})}}, \tag{37}
$$

which indicates the singular behavior of the transition of the gapped phase into the gapless phase. The magnetization shows the square root field dependent behaviour

$$
M^z=\left[\frac{1}{2}g_s+\frac{1}{6}(g_s-g_t)\right]\mu_{\mathrm{B}}+\frac{4Q}{\pi}\left[\frac{1}{2}(g_t+g_s)-\frac{1}{6}(g_s-g_t)\right]\mu_{\mathrm{B}}\left(1-\frac{2Q}{\pi}\right). \tag{38}
$$

If the magnetic field is further increased to $h > 3J_\perp/[(g_t+g_s)-\frac{1}{3}(g_s-g_t)]\,\mu_B$, the state $\psi_{\frac{3}{2}}$ becomes the lowest lying state. Thus in this regime, it is reasonable to choose the basis order as $(\psi_{\frac{3}{2}}, \psi_{\frac{1}{2}}^{(-)}, \psi_{\frac{1}{2}}^{(+)}, \psi_{-\frac{1}{2}}^{(-)}, \psi_{-\frac{1}{2}}^{(+)}, \psi_{-\frac{3}{2}})$. Subsequently, the driving terms are given by

$$
\begin{aligned}
g_1^{(1)} &= -J_\parallel \frac{1}{v^2+\frac{1}{4}} - \frac{3}{2}J_\perp + \left[\frac{1}{2}(g_t+g_s) - \frac{1}{6}(g_s-g_t)\right]\mu_B h,\\
g_1^{(2)} &= \left[\frac{3}{2}J_\perp + \frac{1}{3}(g_s-g_t)\right]\mu_B h,\\
g_1^{(3)} &= -\frac{3}{2}J_\perp + g_s\mu_B h,\\
g_1^{(4)} &= \frac{3}{2}J_\perp - \frac{1}{3}(g_s-g_t)\,\mu_B h,\\
g_1^{(5)} &= \left[\frac{1}{2}(g_t+g_s) + \frac{1}{6}(g_s-g_t)\right]\mu_B h.
\end{aligned}
\tag{39}
$$

As the magnetic field increases beyond the critical point H_{c2}, the groundstate becomes a mixture of the doublet and quadruplet states. Strictly speaking, the doublet component $\psi_{\frac{1}{2}}^{(-)}$ and the quadruplet component $\psi_{\frac{3}{2}}$ compete for the groundstate. Other components of the multiplets are gapfull by virtue of both the rung coupling and magnetic field. As the magnetic field becomes stronger, the probability of the quadruplet component $\psi_{\frac{3}{2}}$ becomes higher. The inflection point at $h_{IP} = 3J_\perp/[(g_t+g_s)-\frac{1}{3}(g_s-g_t)]\,\mu_B$ indicates an equal probability between the components $\psi_{\frac{3}{2}}$ and $\psi_{\frac{1}{2}}^{(-)}$, which can be seen clearly from the magnetization curve in Fig. 4. Using the TBA equations with the driving term (39), we find that for a sufficiently large magnetic field $h \geqslant H_{c3}$ the groundstate becomes fully-polarized with a full saturation magnetization plateau at $M^z = (\frac{1}{2}g_t + g_s)\,\mu_B$. The critical point is given by

$$
H_{c3} = \frac{3J_\perp + 8J_\parallel}{[(g_t+g_s)-\frac{1}{3}(g_s-g_t)]\,\mu_B}. \tag{40}
$$

Analogously, we find the singular behavior in the vicinity of the the critical point H_{c3}. The susceptibility is given by

$$
\chi \approx \frac{3[\frac{1}{2}(g_s+g_t)\,\mu_B - \frac{1}{6}(g_s-g_t)\,\mu_B]^{\frac{3}{2}}}{4\pi\sqrt{J_\parallel(H_{c3}-h)}}, \tag{41}
$$

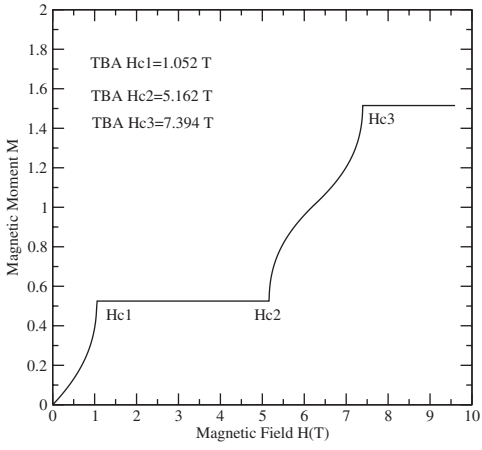

Fig. 4. The magnetization versus magnetic field h in the strong antiferromagnetic rung coupling regime. The magnetic moment is normalized from the magnetization via $M^z/\frac{1}{2}(g_s+g_t)\,\mu_{\rm B}$. The coupling constants used are $J_\perp = 6.0K$, $J_\parallel = 0.4K$ and we take g-factor values $g_s = 2.22$, $g_t = 2.09$ with $\mu_{\rm B} = 0.672K/T$. From the TBA we predict that the one third saturation magnetization plateau opens only if $J_\perp \geqslant J_c^{+F}$ as given in (23). The indicated critical fields $H_{c1} \approx 1.052$ T, $H_{c2} \approx 5.162$ T, and $H_{c3} \approx 7.394$ T predicted by the TBA coincide with the numerically estimated values. The inflection point at $h = h_{\rm IP} \approx 6.278$ T and $M \approx 1$ indicates a point of equal probability for the states $\psi_{\frac{3}{2}}$ and $\psi_{\frac{1}{2}}^{(-)}$.

which indicates the nature of the singular behavior of the transition between the gapless and gapped phases. The magnetization also exhibits the square root field dependent behaviour

$$M^z = \left[\frac{1}{2}g_t + g_s\right]\mu_{\rm B} - \frac{4Q}{\pi}\left[\frac{1}{2}(g_t+g_s) - \frac{1}{6}(g_s-g_t)\right]\mu_{\rm B}\left(1-\frac{2Q}{\pi}\right), \qquad (42)$$

where the Fermi point Q is

$$Q \approx \sqrt{\frac{\left[\frac{1}{2}(g_t+g_s) - \frac{1}{6}(g_s-g_t)\right]\mu_{\rm B}(H_{c3}-h)}{16J_\parallel}}\,. \qquad (43)$$

The magnetization increases almost linearly between the critical fields H_{c2} and H_{c3}.

We have obtained the whole magnetization curve by numerically solving the TBA equations in the different phases (see Fig. 4). A third and full saturation magnetization plateaux is observed. On the other hand, as mentioned above, the first magnetization plateau at $M^z = \frac{1}{2}g_s\mu_{\rm B} + \frac{1}{6}(g_s-g_t)\,\mu_{\rm B}$ depends mainly on the rung coupling. If $J_\perp < J_c^{+F}$ this plateau

disappears. J_c^{+F} is a necessary condition for the existence of the one third saturation magnetization plateau. This conclusion is reasonable because the leg part of the Hamiltonian (1) is stronger than the rung part, due to the multispin interaction terms in Eq. (2). Therefore, the rung coupling must be large enough in order to dominate the low temperature groundstate. If the rung coupling fulfills $J_c^{+} < J_\perp < J_c^{+F}$ the field-induced fractional plateau vanishes. In Fig. 5 we show the full numerical magnetization curve for weak rung coupling $J_\perp = 1.3$ K. We clearly see that the fractional magnetization plateau is closed. From the TBA analysis the first critical point H_{c1} lies in the interval

$$\frac{3(J_\perp - J_c^{+})}{[g_t + 3g_s + (g_s - g_t)/3]\,\mu_B} < H_{c1} < \frac{3J_\perp}{[g_t + 3g_s + (g_s - g_t)/3]\,\mu_B},$$

which for the given parameter set (see figure captions) evaluates to $0.47 < H_{c1} < 0.66$ T. Indeed, from the numerical results we find $H_{c1} \approx 0.605$ T. This implies that for $H < 0.605$ T the groundstate is the doublet spin liquid phase. A magnetic field beyond this point allows the quadruplet component $\psi_{\frac{3}{2}}$ to be involved in the groundstate. Therefore the critical point H_{c1} indicates a quantum phase transition from a two-state phase into a three-state phase. Hence for $h > 0.605$ T, two Fermi seas, $\epsilon^{(1)}$ and $\epsilon^{(2)}$, lie in the groundstate. We can see that the probability of the component $\psi_{\frac{3}{2}}$ to be in

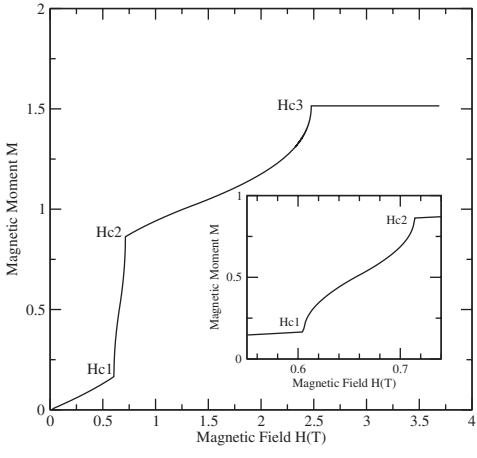

Fig. 5. The magnetization versus magnetic field h in the weak antiferromagnetic rung coupling regime. The numerical values are the same as for the previous figure, but now using the smaller rung coupling constant $J_\perp = 1.3\ \mathrm{K} < J_c^{+F} \approx 2.07$ K. In this case the fractional magnetization plateau vanishes. The TBA critical fields coincide again with the numerically estimated values. The inset shows an enlargement of the magnetization between H_{c1} and H_{c2}.

the groundstate increases as the magnetic field increases. Meanwhile the doublet state $\psi^{-}_{-\frac{1}{2}}$ is quickly driven out of the groundstate at the critical point H_{c2}, where the phase transition from the three-state into the two-state phase occurs. From Eq. (11), we find the middle point between H_{c1} and H_{c2} is approximately at 0.66 T, which is consistent with the numerical curve in Fig. 5. Thus from the theory we predict the critical field to be $H_{c2} = 6J_{\perp}/[(g_t + g_s) - \frac{1}{3}(g_s - g_t)]\,\mu_B - H_{c1} \approx 0.715$ T. This again is in agreement with the numerical value of 0.713 T. In the region $H_{c2} < h < H_{c3}$ the two components $\psi^{-}_{\frac{1}{2}}$ and $\psi_{\frac{3}{2}}$ compete to be in the groundstate. If the magnetic field is strong enough, so that $H > H_{c3}$ where H_{c3} is given by (40), the reference state $\psi_{\frac{3}{2}}$ becomes a true physical groundstate.

5. CONCLUSION

We have investigated the phase diagram of the exactly solved mixed spin-($\frac{1}{2}$, 1) ladder model in both the absence and presence of an external magnetic field using the TBA. It has been shown that in the strong antiferromagnetic rung coupling regime there exists a third and full saturation magnetization plateau. A Luttinger liquid magnetic phase exists in the regime $h < H_{c1}$, which corresponds to the doublet $su(2)$ phase. The magnetic groundstate consisting of two components $\psi^{-}_{\frac{1}{2}}$ and $\psi_{\frac{3}{2}}$ lies in the regime $H_{c2} < h < H_{c3}$. The ferromagnetic ground state with a third saturation magnetization plateau appears in the regime $H_{c1} < h < H_{c2}$. The full saturation magnetization plateau opens at $h > H_{c3}$. The gapped or gapless states appear in turn as the magnetic field is increased. The weak rung coupling regime exhibits three different phase transitions, which involve two- and three-state quantum phase transitions. The fractional magnetization plateau vanishes. The model does not exihibit a third saturation magnetization plateau in the strong ferromagnetic rung coupling regime. We have also investigated the singular behaviour in the vicinity of the critical points via the solutions of the TBA equations. As the contributions from the leg interaction to the groundstate energy are very small in the strong rung coupling regime we believe that the solvable model (1) is well suited to describe the physics of real mixed spin-($\frac{1}{2}$, 1) ladder compounds with a relatively large rung coupling constant. However, such mixed spin ladder compounds are yet to be found.

One compound that we are aware of is the organic ferrimagnet PNNBNO,[31] which has been recognized as a ladder compound with alternating spin-$\frac{1}{2}$ and spin-1 units, i.e., as two coupled alternating mixed spin chains. The strong interchain (rung) coupling suggests that PNNBNO can be effectively identified as a mixed spin-($\frac{1}{2}$, 1) ladder model via the Hamiltonian (1) in the high temperature limit ($T \geqslant 50$ K). In this case the

dominant rung interaction forms an effective one-dimensional spin-$\frac{3}{2}$ antiferromagnetic chain. Of course for low temperatures the ferrimagnetic correlations between the spin-1 and spin-$\frac{1}{2}$ units should appear. Nevertheless we believe that the mixed spin-($\frac{1}{2}$, 1) ladder model discussed here can at least describe the high temperature properties of PNNBNO.[31]

ACKNOWLEDGMENTS

This work has been supported by the Australian Research Council. Z.J.Y. thanks FAPERGS for financial support. N.O. thanks DAAD for financial support. We thank A. Foerster and H.-Q. Zhou for helpful discussions. X.W.G. also thanks the Centre for Mathematical Physics at the University of Queensland for kind hospitality.

REFERENCES

1. E. H. Lieb, *Phys. Rev. Lett.* **18**:692 (1967); *Phys. Rev.* **162**:162 (1967).
2. E. Dagotto and T. M. Rice, *Science* **271**:618 (1996); E. Dagotto, *Rep. Prog. Phys.* **62**:1525 (1999).
3. M. Azuma, Z. Hiroi, M. Takano, K. Ishida, and Y. Kitaoka, *Phys. Rev. Lett.* **73**:3463 (1994).
4. B. Chiari, O. Piovesana, T. Tarantelli, and P. F. Zanazzi, *Inorg. Chem.* **29**:1172 (1990); G. Chaboussant *et al.*, *Phys. Rev. Lett.* **79**:925 (1997); M. Hagiwara, A. Katori, U. Schollwöck, and H.-J. Mikeska, *Phys. Rev. B* **62**:1051 (2002).
5. B. C. Watson, V. N. Kotov, and M. W. Meisel, *Phys. Rev. Lett.* **86**:5168 (2001).
6. C. P. Landee, M. M. Turnbull, C. Galeriu, J. Giantsidis, and F. M. Woodward, *Phys. Rev. B* **63**:100402 (2001).
7. H. Tanaka, K. Takatsu, W. Shiramura, and T. Ono, *J. Phys. Sci. Japan* **65**:1945 (1990); W. Shiramura, K. Takatsu, H. Tanaka, K. Kamishima, M. Takahashi, H. Mitamura, and T. Goto, *J. Phys. Soc. Japan* **66**:1900 (1997); N. Gavadini, W. Henggeler, A. Furrer, H.-U. Güdel, K. Krämer, and H. Mutka, *Eur. Phys. J. B* **7**:519 (1999).
8. E. Dagotto, J. Riera, and D. J. Scalapino, *Phys. Rev. B* **45**:5744 (1992); S. Gopalan, T. M. Rice, and M. Sigrist, *Phys. Rev. B* **49**:8901 (1994).
9. A. A. Nersesyan and A. M. Tsvelik, *Phys. Rev. Lett.* **78**:3939 (1997); A. K. Kolezhuk and H.-J. Mikeska, *Phys. Rev. Lett.* **80**:2709 (1998); T. Giamarchi and A. M. Tsvelik, *Phys. Rev. B* **59**:11398 (1999).
10. T. Barnes and J. Riera, *Phys. Rev. B* **50**:6817 (1994); K. Hida, *Phys. Rev. B* **46**:8268 (1992).
11. G. S. Uhrig and B. Normand, *Phys. Rev. B* **58**:R14705 (1998).
12. W. Zheng, R. R. P. Singh, and J. Oitmaa, *Phys. Rev. B* **55**:8052 (1997); X. Wang and L. Yu, *Phys. Rev. Lett.* **84**:5399 (2000).
13. M. Reigrotzki, H. Tsunetsugu, and T. M. Rice, *J. Phys. Condens. Matter* **6**:9235 (1994).
14. G. Chaboussant, M.-H. Julien, Y. Fagot-Revurat, M. Hanson, L. P. Lęvy, C. Berthier, M. Horvatiç, and O. Piovesana, *Eur. Phys. J. B* **6**:167 (1998).
15. M. Troyer, H. Tsunetsugu, and D. Würtz, *Phys. Rev. B* **50**:13515 (1994).
16. Y. Wang, *Phys. Rev. B* **60**:9236 (1999); Y. Wang and P. Schlottmann, *Phys. Rev. B* **62**:3845 (2000).
17. H. Frahm and A. Kundu, *J. Phys. C: Cond. Mat.* **11**:L557 (1999).

18. M. T. Batchelor and M. Maslen, *J. Phys. A* **32**:L377 (1999); J. de Gier, M. T. Batchelor, and M. Maslen, *Phys. Rev. B* **61**:15196 (2000); J. de Gier and M. T. Batchelor, *Phys. Rev. B* **62**:R3584 (2000); M. T. Batchelor, J. de Gier, J. Links, and M. Maslen, *J. Phys. A* **33**:L97 (2000); M. Maslen, M. T. Batchelor, and J. de Gier, *Phys. Rev. B* **68**:024418 (2003).
19. M. T. Batchelor, J. de Gier, and M. Maslen, *J. Stat. Phys.* **102**:559 (2001).
20. J. Links and A. Foerster, *Phys. Rev. B* **62**:3845 (2000); A. Foerster, K. E. Hibberd, J. R. Links, and I. Roditi, *J. Phys. A* **34**:L25 (2001).
21. A. A. Zvagin, *J. Phys. A* **34**:R21 (2001); D. Arnaudon, A. Sedrakyan, and T. Sedrakyan, preprint, hep-th/0210087.
22. M. T. Batchelor, X.-W. Guan, A. Foerster, and H.-Q. Zhou, *New J. Phys.* **5**:107 (2003); M. T. Batchelor, X.-W. Guan, A. Foerster, and H.-Q. Zhou, *Nucl. Phys. B* **669**:385 (2003).
23. K. Kodma and M. Takigawa *et al.*, *Science* **298**:395 (2002).
24. A. K. Kolezhuk, H.-J. Mikeska, and S. Yamamoto, *Phys. Rev. B* **55**:R3336 (1997); A. K. Kolezhuk, H.-J. Mikeska, K. Maisinger, and U. Schollwöck, *Phys. Rev. B* **59**:13565 (1999).
25. S. Yamamoto, *Phys. Rev. B* **59**:1024 (1999); S. Yamamoto and T. Sakai, *J. Phys.: Condens. Matter* **11**:5175 (1999).
26. S. K. Pati, S. Ramasesha, and D. Sen, *Phys. Rev. B* **55**:8894 (1997); T. Sakai and K. Okamoto, cond-mat/0204375.
27. W. Zheng and J. Oitmaa, cond-mat/0301580.
28. J. Lou, C. Chen, and S. Qin, *Phys. Rev. B* **64**:144403 (2001).
29. M. Hagiwara, K. Minami, Y. Narumi, K. Tatani, and K. Kindo, *J. Phys. Soc. Japan* **67**:2209 (1998).
30. K. Takano, *Physica B* **329**:1271 (2003); J.-H. Park *et al.*, *Physica B* **329**:1152 (2003).
31. Y. Hosokoshi, K. Katoch, Y. Nakazawa, H. Nokano, and K. Inoue, *J. Amer. Chem.* **123**:7921 (2001); Y. Hosokoshi, K. Katoch, and K. Inoue, *Synthetic Metals* **527**:133–134 (2003).
32. Y.-Q. Li, M. Ma, D. N. Shi, and F. C. Zhang, *Phys. Rev. Lett.* **81**:3527 (1998); S.-J. Gu and Y.-Q. Li, *Phys. Rev. B* **66**:092404 (2002); S.-J. Gu, Y.-Q. Li, and H.-Q. Zhou, cond-mat/0308432.
33. Z.-J. Ying, A. Foerster, X.-W. Guan, B. Chen, and I. Roditi, cond-mat/0308443.
34. B. Sutherland, *Phys. Rev. B* **12**:3795 (1975); P. Schlottmann, *Phys. Rev. B* **45**:5293 (1992).
35. M. Takahashi, *Prog. Theor. Phys.* **46**:401 (1971); P. Schlottmann, *Phys. Rev. B* **33**:4880 (1986).
36. K. Lee, *J. Korean Phys. Soc.* **27**:205 (1994).
37. H. Kageyama *et al.*, *Phys. Rev. Lett.* **82**:3168 (1999); S. Miyahara and K. Ueda, *Phys. Rev. Lett.* **82**:3701 (1999).